*Mapana – Journal of Sciences*
2026, Vol. 25, No. 2, *41 - 59*
ISSN 0975-3303 | https://doi.org/10.12723/mjs.77.3

# Experimental and Computational Studies on Photophysical Properties of 1-(3-Iodophenoxy methyl)-Benzo[f]Chromen-3-one by Solvatochromic Approaches

Alageri Lingappa [*], Shivaleela Basavaraj[*], Manjula K[*], J. Thipperudrappa[†], S.M. Hanagodimath[*]

## Abstract

The iodinated derivative **13IBC3** was synthesized and its photophysical properties were studied in polar and nonpolar solvents. The ground- and excited-state dipole moments were estimated using equations. Results showed a bathochromic shift with increasing solvent polarity, indicating a larger excited-state dipole moment ($\mu_e > \mu_g$). The change in dipole moment ($\Delta\mu$) was 6.92D (DFT method) and 7.12D (Semiempirical method). The Kamlet and Catalan multiple linear regression analysis revealed that solvent dielectric constants and polarizability significantly influence spectral characteristics. The excited state exhibits intramolecular charge-transfer (ICT) character. Polar solvents alter the fluorescence properties of coumarin. The computational study was carried out with the Gaussian 16W program using the B3LYP. UV-visible spectra of solvated species were calculated using TD-DFT, which confirmed the experimental findings and provided insights into HOMO-LUMO energies, ESP maps, and nonlinear optical properties. The change in dipole moment matched the experimental value.

**Keywords:** DFT structure, LUMO and HOMO, absorption spectra, fluorescence spectra, EPS, dipole moments.

* Department of Physics, Gulbarga University, Kalaburagi, Karnataka, India; alagerilingappa@gmail.com; shivaleelabphysics@gmail.com; smh math@rediffmail.com

† Department of Physics, Vijayanagara Sri Krishnadevaraya University, Ballari, Karnataka, India

## 1. Introduction

Coumarin derivatives are significant oxygen-containing heterocyclic compounds and represent important structural motifs in natural benzopyrone products. They are widely known for their diverse biological activities, including anticancer, antituberculosis, anti-inflammatory, antioxidant, antimalarial, anti-HIV, and antimicrobial effects. In recent years, cancer has emerged as a major cause of mortality and remains a largely incurable disease affecting multiple organs of the human body [1, 2]. Owing to their broad range of biological activities, structural adaptability, and favourable pharmacokinetic profiles, coumarin derivatives play a crucial role in medicinal chemistry. Their importance stems from their role as key molecular frameworks, offering a broad pharmacological spectrum, ease of chemical modification, strong potential as drug leads or scaffolds, and compatibility with modern drug design strategies [3, 4]. These compounds continue to drive the development of next-generation therapeutic diseases. In iodinated coumarin derivatives with biological activity, iodine serves as a heavy halogen, increasing molecular lipophilicity and thereby enhancing drug absorption and improving binding affinity for hydrophobic regions of enzymes and receptors without activating them, ultimately contributing to notable anticancer and antitubercular properties [5].

We have studied the **13IBC3** molecule, a member of a series of iodinated 3-aryloxymethyl coumarins. The dipole moments of the **13IBC3** molecule were evaluated by the solvatochromic method. Stokes shift was determined by using Molecular absorption and emission spectra. A bathochromic (red) shift signifies positive solvatochromism and depends on the nature of solute–solvent interactions. When a solute is introduced into a solvent cavity, its ground state becomes stabilised. If the dipole moment of the solute increases upon electronic excitation, the excited state is partially stabilised by the surrounding solvent dipoles. As the polarity of the solvent increases, a bathochromic (red) shift is observed because the excited state experiences greater stabilisation than the ground state, indicating a higher polarity of the excited state. In contrast, if the dipole moment of the solute decreases during electronic excitation, the excited state is less effectively stabilised due to the unfavourable alignment of solvent dipoles within the cavity. With increasing solvent polarity, a hypochromic (blue) shift occurs. This suggests that the ground state possesses a greater dipolar character than the excited state [6]. In this study, the ground and excited state dipole moments of **13IBC3** were experimentally determined using the Lippert, Kawaski-Chamma-Villet, and Bakhshiev equations with polar and nonpolar solvents." A theoretical quantum-computational study was conducted using Gaussian 16. The

dipole moment, Mulliken charges, HOMO-LUMO molecular orbital energies, electrostatic potential map (ESP), and nonlinear optical properties of the molecule were studied with optimised geometry using density functional theory. The UV-Visible spectra were estimated theoretically using TD-DFT in solvents [7].

## 2. Materials and Methods

### 2.1 DFT Structure of 13IBC3

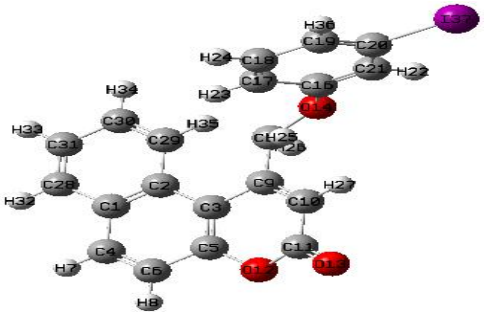


**Figure 1**: DFT Structure of 13IBC3

The molecular structure of **13IBC3** is shown in (Figure 1). We used alcohol from Methanol, Ethanol, Propanol, Pentanol and Hexanol and some general solvents like Acetonitrile, Chloroform, Benzene, DMSO (Dimethyl sulfoxide) and Toluene.

### 2.2 Optimised Vector (OPT-Vector) of 13IBC3

Optimized geometry of **13IBC3** is shown in Figure 2. The arrow mark indicates direction of dipole moment of the molecule.

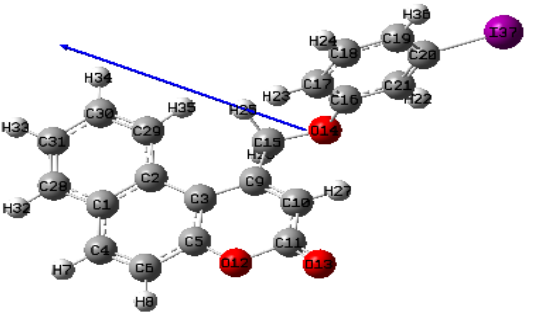


**Figure 2**: OPT Vector of 13IBC3

The gaussian 16 program was used for geometry optimisation from

the Semi- empirical method at the PM6 basis set. Theoretical calculations of HOMO-LUMO and ESP maps were drawn using TD-DFT approaches.

## 2.3 Core Molecular Features

- Formulae: $C_{20}H_{13}IO_3$.
- Exact Mass: 376.9675 g/mol.
- Molar Mass: 377.16 g/mol.
- Double Bond Equivalents (DBE): 11.
- Log P: 4.2 (estimated) [8].

| Feature | Description |
|---|---|
| Ring system | Benzopyrone, chromone |
| Substituents | Iodophenoxymethyl |

## 2.4 Electrostatic potential surface

Electrostatic potential (ESP) maps provide insight into charge distribution, with different colours indicating varying potentials [9, 10]. The maximum red value is -6.248 a.u., and the maximum blue value is +6.248 a.u. The different electrostatic potential values are displayed in different colours. The figure shows the total electron density, with potential regions for electron transitions and reactivity sites indicated by yellow (positive phase) and red (negative phase) contours [11, 12].

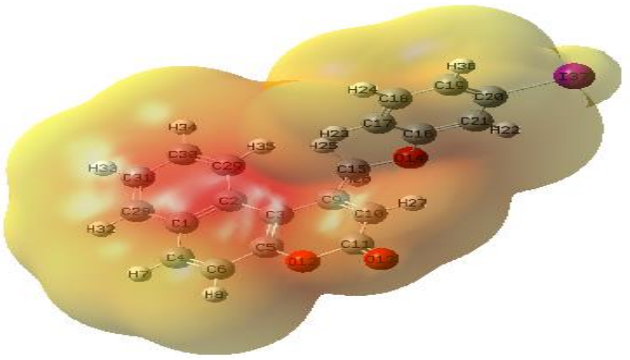

**Figure 3**: EPS of 13IBC3

# 3 Theoretical background

## 3.1 Equations for the estimation of dipole moments

The independent equations used for the estimation of ground and excited state dipole moments in various solvents with varied dielectric constant (ε) and refractive index (n) are as follows [13, 14],

Lippert-Mataga equation- $\bar{\nu}_a - \bar{\nu}_f = m_1 f_1(\varepsilon, n) + Constant$

Bakhshiev's equation - $\bar{\nu}_a - \bar{\nu}_f = m_2 f_2(\varepsilon, n) + Constant$

Kawski-Chamma-Viallet's equation,

$$\frac{\bar{\nu}_a + \bar{\nu}_f}{2} = -m_3 f_3(\varepsilon\ n) + Constant$$

Where $\bar{\nu}_a$ and $\bar{\nu}_f$ are absorption and emission maxima wave numbers in $cm^{-1}$[15].

## 3.2 Estimation of dipole moments

The $\mu_e$ **The 13IBC3 molecule was determined by using the** Lippert-Mataga equation, Bakshiev's, and Kawski-Chamma-Viallet's relations. Using these polarity parameters, the following expressions can be obtained to estimate $\mu_e$ and $\mu_g$ [16, 17].

$$\mu_g = \frac{m_2 - m_1}{2}\left(\frac{hca^3}{2m_1}\right)^{1/2} \mu_g = \frac{m_2 + m_1}{2}\left(\frac{hca^3}{2m_1}\right)^{1/2}$$

Slopes $m_1$ and $m_2$ have got from the plots of $(\bar{\nu}_a - \bar{\nu}_f)$ v/s $f_1(\varepsilon\ n)$, and $\frac{\bar{\nu}_a + \bar{\nu}_f}{2}$ versus $f_2(\varepsilon\ n)$ for different solvents, respectively. Where '**h' is** Planck's constant, **c** is the velocity of light and 'a ' is the Onsager cavity radius of a molecule.

If $\mu_e$ and $\mu_g$ are not parallel to one another, then the angle ϕ between $\mu_e$ and $\mu_g$ can be estimated using the below (2) [18]

$$\cos \emptyset = \frac{1}{2\mu_g \mu_e}\left[\left({\mu_g}^2 + {\mu_e}^2\right) - \frac{m_2}{m_1}\left({\mu_e}^2 - {\mu_g}^2\right)\right]$$

The $\mu_e$ is also estimated by means of $E_N^T$using the below

$$\left(\bar{\nu}_a - \bar{\nu}_f\right) = 11307.6\left[\left(\frac{\Delta\mu}{\Delta\mu_s}\right)^2\left(\frac{a_s}{a}\right)^3\right] E_N^T + Constant$$

Where $'\Delta\mu_B'$ is the change in dipole moment, $'a_S'$ is the Onsager radius of the solvent Δμ, and a are the corresponding parameters of the compound [19].

### 3.3 Lippert equation

The Lippert equation describes the interactions between solutes and solvents. The equation is as follows

$$hc\Delta\bar{\nu} = hc\,(\overline{\nu_a} - \overline{\nu_a}) = \frac{2\Delta f}{a^3}\,(\mu_E - \mu_G)^2 + Constant$$

Where $\Delta\boldsymbol{\nu}$ is the frequency shift ($cm^{-1}$) between absorption and emission. $\Delta f$ is orientation polarizability. In contrast, the new excited-state dipole forms during this timespan, while the surrounding solvent molecules do not immediately reorient. Because of the relatively long lifetime of the excited state ($10^{-8}$ s), solvent molecules can orient to their equilibrium positions around the fluorophore prior to emission [20, 21, 22].

The energy of the dipole in an electric field is given by

$$F_{dipole} = -\mu R$$

Where 'R' is the electric field. The reactive field is parallel and opposite to the direction of the dipole, and is proportional to the magnitude of the dipole moment [23, 24].

$$R = \frac{2\mu}{a^3} f$$

Where '$f$'is the polarizability of the solvent and 'a' is the cavity radius. The high-frequency polarizability *f(n)* depends on the refractive index [25].

$$\text{f(n)} = \frac{n^2-1}{2n^2+1}$$

The solvent's polarizability also depends on its dielectric constant, which accounts for the orientation of solvent molecules. The low-frequency polarizability of the solvent is expressed as:

$$f(\varepsilon) = \frac{\varepsilon - 1}{2\varepsilon + 1}$$

The difference between $f(\varepsilon)$ and f(n)

$$\Delta f = \frac{\varepsilon - 1}{2\varepsilon + 1} - \frac{n^2 - 1}{2n^2 + 1}$$

This is called orientation polarizability. The electronic motions ($R_{el}^G$, $R_{el}^E$) and those due to solvent reorientation ($R_{or}^G$, $R_{or}^E$). Understanding that equilibrium around dipole moments of the ground states, these reactive fields are given by

$$R_{el}^G = \frac{2\mu_G}{a^3} f(n) \qquad R_{el}^E = \frac{2\mu_E}{a^3} f(n)$$

$$R_{or}^G = \frac{2\mu_G}{a^3} \Delta f \qquad R_{or}^E = \frac{2\mu_E}{a^3} \Delta f$$

For absorption of light, the energies of the ground ($E^G$) and nonequilibrium excited ($E^E$) states are

$$\text{Energy}^E \text{ (absorption)} = E_V^E - \mu_E R_{or}^G - \mu_E R_{el}^E$$

$$\text{Energy}^G \text{ (absorption)} = E_V^E - \mu_G R_{or}^G - \mu_G R_{el}^G$$

Here, EV represents the energy levels of the fluorophore in the vapour state. The absorption transition energy is decreased by the electron reaction because the electrons in the solvent can follow the rapid change in electron distribution within the fluorophore [26, 27]. The effect of the orientation polarizability, given $\mu_G R_{or}^G$ and $\mu_E R_{or}^G$, contains only the ground state orientational reaction field. This separation of effects is due to the Franck-Condon principle.

Energy is related to the wavelength and is given by $= \frac{\Delta E}{hc}$.

Energy of absorption

$$hc\,\nu_A = hc\,(\nu_A)_V - (\mu_E - \mu_G)\,(R_{or}^G) - \mu_E R_{el}^E + \mu_G R_{or}^G$$

For emission, the energy of the two electronic levels

$$\text{Energy}^E \text{ (emission)} = E_V^E - \mu_E R_{or}^G - \mu_E R_{el}^G$$

$$\text{Energy}^G \text{ (emission)} = E_V^G - \mu_G R_{or}^E - \mu_G R_{el}^G$$

The energy of the emission is given by

$$hc\bar{\nu}_f = hc(\bar{\nu}_f)_V - (\mu_E - \mu_G)R_{or}^E - \mu_E R_{el}^E + \mu_G R_{el}^G$$

$\bar{\nu}_a - \bar{\nu}_f$ is constant for complex molecules,

$$\bar{\nu}_a - \bar{\nu}_f = -\frac{1}{hc}(\mu_E - \mu_G)(R_{or}^G - R_{or}^E) + constant$$

But $\quad R_{or}^G = \frac{2\mu_G}{a^3}\,\Delta f \qquad R_{or}^E = \frac{2\mu_E}{a^3}\,\Delta f$

Then, $\quad \bar{\nu}_a - \bar{\nu}_f = \frac{-2}{hca^3}(\mu_E - \mu_G)(\mu_G \Delta f - \mu_E\,\Delta f) + constant$

$$\bar{\nu}_a - \bar{\nu}_f = \frac{2\Delta f}{hca^3}(\mu_E - \mu_G)^2 + constant$$

The Lippert equation is only an approximation and contains many assumptions. The fluorophore is assumed to be spherical, and there is no consideration of specific interactions with the solvent.

The Lippert equation states that the ground and excited states' dipole moments point in the same direction. If one assumes the polarizability of the fluorophore is the same as the solvent, and that $\mu_G$ and $\mu_E$ point in different directions, then if these directions are different, the Lippert equation becomes [28].

$$hc\Delta\bar{\nu} = \Delta b\left[\frac{\varepsilon-1}{\varepsilon+2} - \frac{n^2-1}{n^2+2}\right]\frac{(2n^2+1)}{(n^2+2)} + constant$$

Where,

$$\Delta \boldsymbol{b} = \frac{\mathbf{2}}{\boldsymbol{hca^3}}\left(\mu_G{}^2 - \mu_E{}^2 - \mu_G\mu_E\cos\alpha\right)$$

and $\alpha$ is the angle between $\mu_G$ *and* $\mu_E$.

It is reasonable to expect that the solvent effect depends on the angle between $\mu_G$ *and* $\mu_E$. However, for many fluorophores, dipole moments in the ground and excited states are oriented in similar directions. Despite this, significant spectral shifts are often observed due to specific solvent interactions. Therefore, it is more appropriate to apply the Lippert equation when interpreting this spectral analysis. Derivation from the predicted behaviour can indicate the presence of additional interactions [29].

# 4 Results and Discussion

## 4.1 Photophysical Properties

- UV-VIS Absorption: The dominant π–π* band typically appears at 300-380 nm, with the maximum ($\lambda_{max}$) shifting to ~310 nm due to electron-donating substituents and extended conjugation [30].
- Emission: The compound emits in the blue-green range (400–520 nm), where emission shows red shift in polar solvents, and the Stokes shift is moderate (90–150 nm).
- Quantum Yield ($\Phi_f$): It is predicted to be 0.28–0.48; higher in non-protic, rigid media and lower with H-bonding or quenching processes [31].
- Lifetime ($\tau_f$): It is ~1.2–2.5 ns in an air-saturated solution

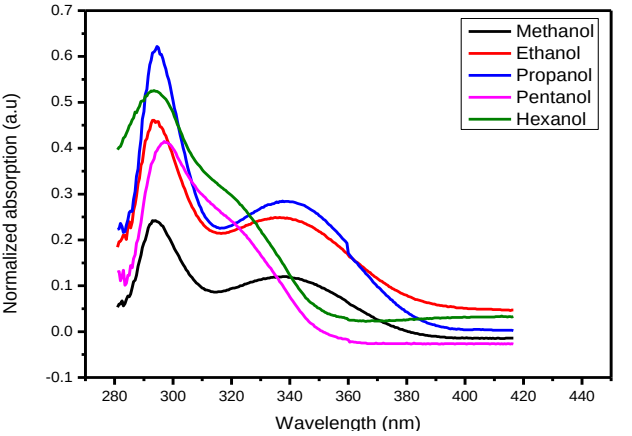


**Figure 4:** Absorption spectra of **13IBC3** in polar solvents

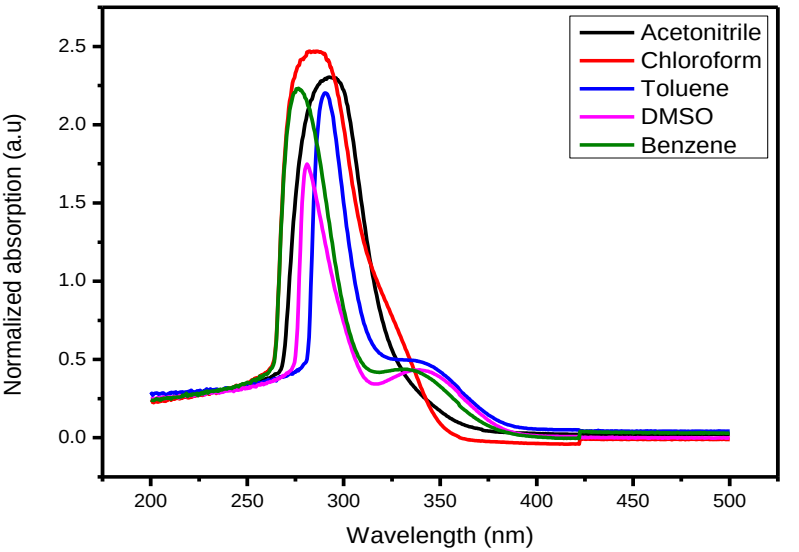


**Figure 5:** Absorption spectra of **13IBC3** in nonpolar solvents

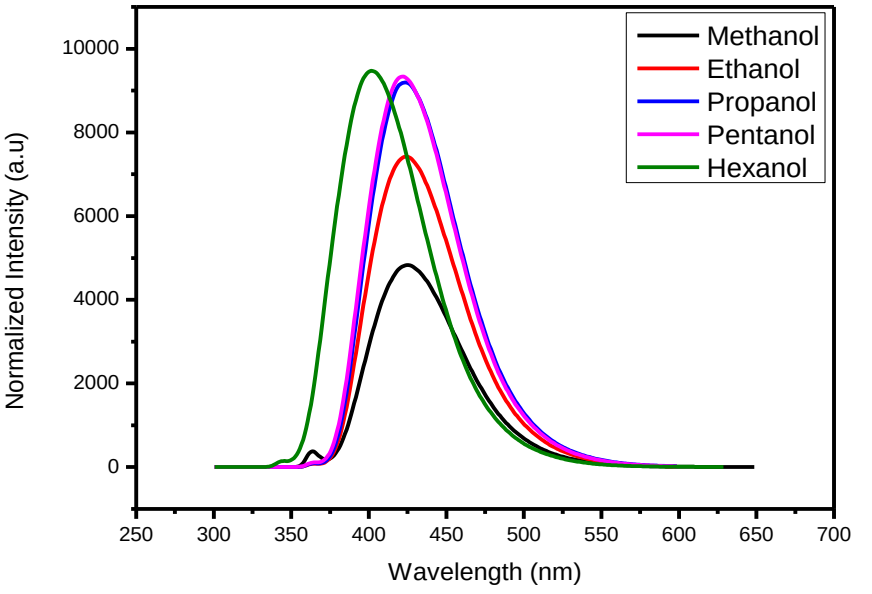


**Figure 6:** Fluorescence spectra of **13IBC3** in polar solvents

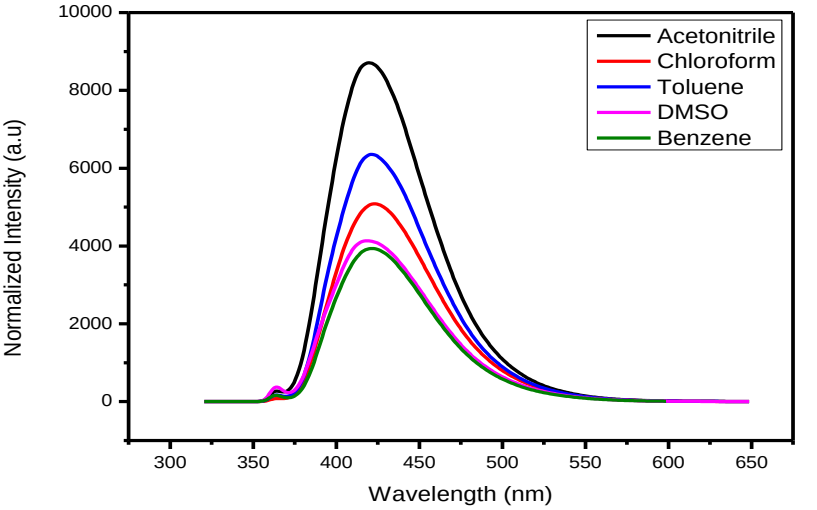


**Figure 7:** Fluorescence spectra of **13IBC3** in nonpolar solvents

## 4.2 HOMO and LUMO of 13IBC3

**HOMO** **LUMO**

$E_{HOMO}$ = -0.341 *eV* $E_{LUMO}$ = -0.053 *eV*

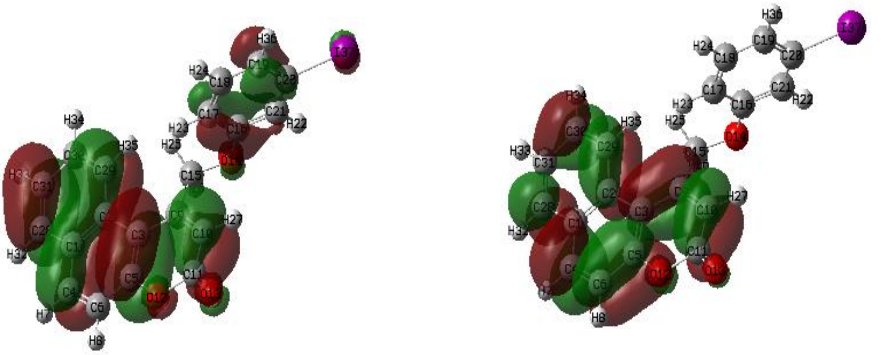

**ΔE = -0.228 eV**

**Figure 8:** HOMO and LUMO of **13IBC3**

The charge distribution and photophysical properties of 13IBC3 have been investigated using molecular orbital calculations. The energy absorption of electrons, or the transition from the ground state to the first excited state, is essentially described by one electron excitation from the highest occupied molecular orbital to the lowest empty molecular orbital. The term "HOMO-LUMO energy gap" describes the difference in energy between HOMO and LUMO. The energy difference between these border orbitals is used as an analytical measure to understand and model molecular transport properties.

The geometry of the **13IBC3** fluorophore was optimised using the DFT method B3LYP/6-31+G (d, p). The ground-state dipole moment is 6.92 Debye. The molecular orbital surfaces for HOMO and LUMO are shown. These orbitals are crucial in determining a molecule's chemical reactivity and stability [32, 33]. A smaller HOMO–LUMO energy gap signifies enhanced molecular stability, which leads to a change in dipole moment due to the redistribution of electron density. The HOMO and LUMO energies in the gas phase are −0.341 eV and −0.053 eV. yielding an energy gap of 0.288 eV. This relatively small gap, along with high chemical softness, indicates that the molecule is soft and highly polarizable. Furthermore, electronegativity leads to an asymmetric distribution of electron density, and the chemical potential reflects the tendency of electrons to escape from the system, thereby indicating lower electrophilicity [34, 35].

**Table 1**: Solvent polarity parameter values

$\boldsymbol{\lambda_a - \lambda_f}$, $\boldsymbol{\lambda_a + \lambda_f}$, $\frac{\boldsymbol{\lambda_a + \lambda_f}}{2}$, $\frac{\boldsymbol{\lambda_a - \lambda_f}}{2}$, $\boldsymbol{\nu_a + \nu_f}$, $\boldsymbol{\nu_a - \nu_f}$, $\frac{\boldsymbol{\nu_a + \nu_f}}{2}$ and $\frac{\boldsymbol{\nu_a - \nu_f}}{2}$

| **Solvents** | $\boldsymbol{\lambda_a - \lambda_f}$ | $\boldsymbol{\lambda_a + \lambda_f}$ | $\frac{\boldsymbol{\lambda_a + \lambda_f}}{2}$ | $\frac{\boldsymbol{\lambda_a - \lambda_f}}{2}$ | $\boldsymbol{\nu_a + \nu_f}$ | $\boldsymbol{\nu_a - \nu_f}$ | $\frac{\boldsymbol{\nu_a + \nu_f}}{2}$ | $\frac{\boldsymbol{\nu_a - \nu_f}}{2}$ |
|---|---|---|---|---|---|---|---|---|
| Methanol | 132 | 718 | 359 | 66 | 1726214 | 315768 | 863107 | 157884 |
| Ethanol | 130 | 718 | 359 | 65 | 1726431 | 312659 | 863215 | 156329 |
| Propanol | 129 | 717 | 358.5 | 64.5 | 1726762 | 309648 | 863381 | 154824 |
| Pentanol | 124 | 718 | 359 | 62 | 1720195 | 296349 | 860097 | 148174 |
| Hexanol | 109 | 695 | 347.5 | 54.5 | 1712096 | 329410 | 856048 | 164705 |
| Acetonitrile | 128 | 712 | 356 | 64 | 1735348 | 308110 | 867674 | 154055 |
| Chloroform | 138 | 710 | 355 | 69 | 1753564 | 339792 | 876782 | 169896 |
| Toluene | 131 | 711 | 355.5 | 65.5 | 1743434 | 319588 | 871717 | 159794 |

| | | | | | | | | |
|---|---|---|---|---|---|---|---|---|
| DMSO | 137 | 699 | 349.5 | 68.5 | 1782170 | 348104 | 891085 | 174052 |
| Benzene | 145 | 699 | 349.5 | 72.5 | 1791553 | 371081 | 895776 | 185540 |

The absorption maximums, emission maximums, wavenumbers, Stokes shift, and arithmetic mean values for a 13IBC3 in general solvents and alcohols are listed in Table 1. The emission spectra of 13IBC3 in general solvents and alcohols were shown in Figures 6 and 7. The shift in the peaks of the emission spectrum is due to the bathochromic transition.

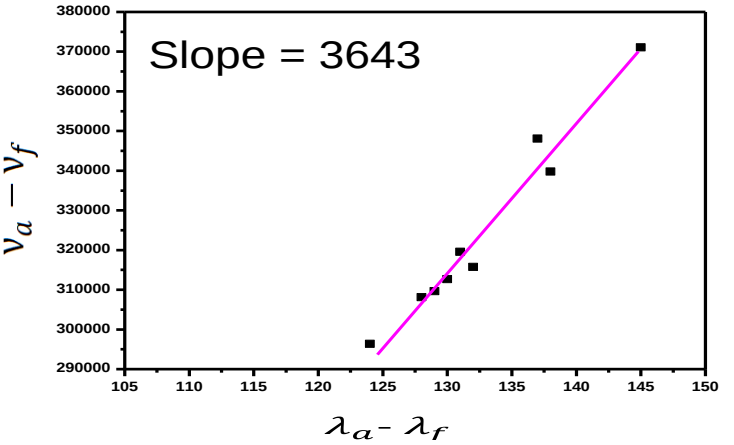


**Figure 9:** Stoke's Shift, $\nu_a - \nu_f$ Vs $\lambda_a - \lambda_f$ of **13IBC3**

The Lippert–Mataga graph of 13IBC3 is presented in Figure 9. The Stokes shift is plotted against the solvent polarity function, a straight line with a good correlation coefficient.

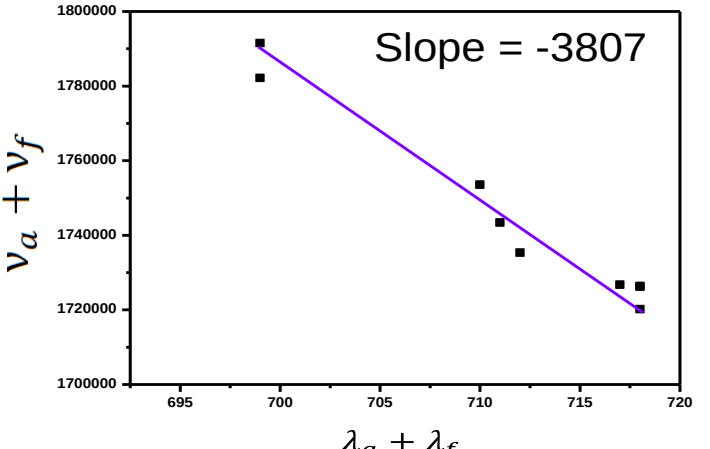


**Figure 10:** Graph of $\nu_a + \nu_f$ Vs $\lambda_a + \lambda_f$ of **13IBC3**

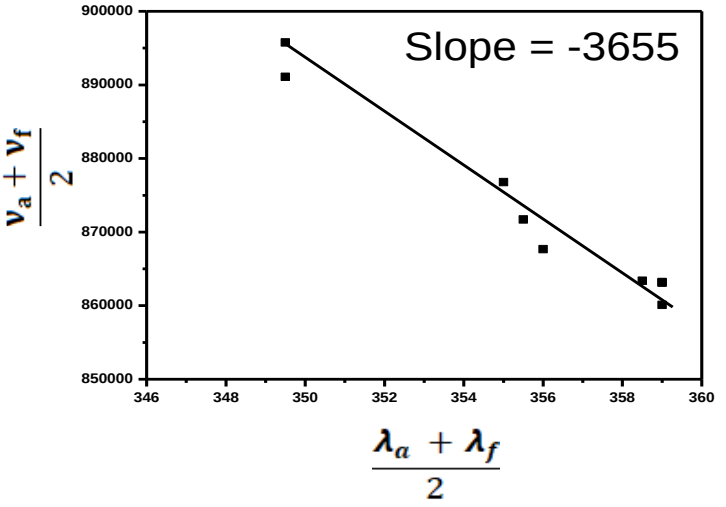


**Figure 11**: Lippert-Mataga graph of 13IBC3, $\frac{\nu_a+\nu_f}{2}$ *Vs* $\frac{\lambda_a+\lambda_f}{2}$

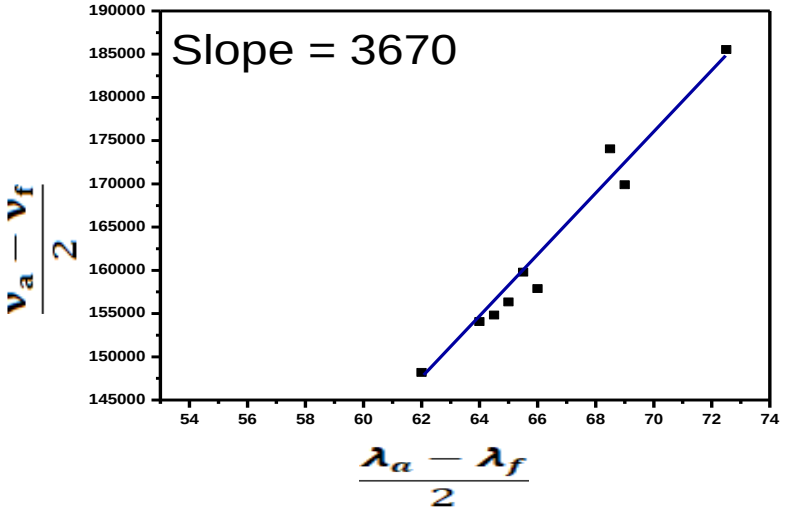


**Figure 12**: Stoke's Shift of 13IBC3, $\frac{\nu_a-\nu_f}{2}$ *Vs* $\frac{\lambda_a-\lambda_f}{2}$

Figures 7 and 8 show plots of Stoke's shift versus the polarity function. The graphs were used to calculate the slopes for the Bakshiev and Lippert-Mataga methods. According to the J T Edward technique, the radius of the 4MPDC molecule is 3.98 Å. The ground state dipole moment for the Lippert and Bakshiev methods was found to be 1.99 D, and the excited state dipole moment was found to be 4.06 D and 5.31 D, respectively.

According to the computations, the dipole moment values of the excited state are greater than those of the ground state.

### 4.3 Structure and Evidence

**Lactone carbonyl:**

Strong doublets around 1720 $cm^{-1}$ (conjugated C=O) and 1810 $cm^{-1}$ (lactone C=O). Indicates coumarin-type core; lower C=O due to aromatic conjugation [36].

**Fingerprint region:**

Rich, complex, indicative of multiple ring systems and ether linkages [37].

**Recommended Checks:**

Compare experimental spectrum with DFT-computed IR: Use a scaling factor (≈0.96–0.99) to match peak assignments to normal modes for confirmation.

Additional spectra (e.g., Raman, isotope labelling): Can help refine assignments of C–H, C–O, and aromatic vibrations [38].

## 5 Results from Computation

The DFT/B3LYP/6-311G method is used to obtain optimised ground-state geometry, ground- and excited-state dipole moments, absorption and fluorescence maxima in nm, and the HOMO-LUMO gap in eV [39].

DFT studies of 13IBC3 provide valuable insights into its electronic, structural, and photophysical properties. It gives an idea about the Prediction of its reactivity and interactions with biomolecules, and the development of new coumarin derivatives with improved performance [40].

## 6 Summary

The fluorescent molecule 13IBC3 features an extensive conjugated structure, which gives rise to unique photophysical and nonlinear optical properties. Its intense absorption and adjustable emission, together with sensitivity to the surrounding environment and distinct IR features, are a result of its expanded aromatic framework and varied functional groups. The distribution of charge, dipole moment, and hyperpolarizability emphasises its suitability for nonlinear optical and sensing applications. Moreover, its properties can be reliably studied through UV–Vis spectroscopy. Overall,

strong fluorescence, significant polarizability, and excellent photostability make it well-suited for applications in advanced imaging, sensing, and optoelectronic devices.

## 7 Conclusion

The ground- and excited-state dipole moments of the iodinated coumarin derivative of molecule 13IBC3 were studied in polar and nonpolar solvents. From the experimental and theoretical methods, observed that the excited-state dipole moment is greater than the ground-state dipole moment. The bathochromic shift observed as solvent polarity increases indicates positive Solvatochromism. Polar solvents stabilise the charge transfer excited state, resulting in red-shifted emission, and induce a strong $\pi \; to \; \pi^*$ transition. In a computational study using TD-DFT, the UV- visible spectra indicate that the dipole moments in the excited state are greater than those in the ground state, particularly in the presence of solvents. The small energy indicates an easier electron transfer from the HOMO to LUMO, and it is soft and highly polarizable. The ESP surfaces provide details regarding a molecule's partial charges, electron density, and electron negativity. Numerous possible uses for these photophysical characteristics exist in the biological and pharmacological fields.

## 8 Authorship contribution statement

**Alageri Lingappa:** Completed the computational and experimental portions and wrote the manuscript. **Shivaleela B and J. Thipperudrappa:** made a significant contribution to the data preparation, **Manjula K:** Title coumarin fluorescence organic compound synthesis, **S.M. Hanagodimath:** Supervised all of the work.

## 9 Declaration of competing interest

The author declares that they have no known competing financial interests or personal relationships that could have influenced the results reported in this paper.

## 10 Funding

No significant support from any scientific organisation has been provided to the authors.

## 11 Section snippets: Reagents and apparatus

Sigma-Aldrich and S.D. Fine Chemicals Ltd., India, provided the spectroscopic-grade chemicals and solvents. A spectrofluorophotometer at

USIC, Karnataka University and a UV–visible spectrophotometer at USIC, Gulbarga University were used to record the absorption and fluorescence spectra at room temperature. To reduce self-absorption, sample solutions ($10^{-5}$ M) were made in solvents with different polarities.

## 12 Acknowledgement

We are grateful to the director and technical personnel of USIC, Gulbarga University, Kalaburagi, and USIC, Karnataka University, Dharwad, for donating the Spectro fluorophotometer.

## References

[1]. Asnaashari M, Kenari RE, Taghdisi SM, Abnous K, Farahman dfar R (2024) A novel fluorescent DNA sensor for acrylamide detection in food samples based on Single-Stranded DNA and gelred. J Fluoresc 34:2845–2860, https://doi.org/10.1007/s10895- 023-03479-7.

[2]. Erdemir GY, Topkaya D (2024) Synthesis, characterization and evalua ting photochemical properties of Porphyrin-substituted Azobenzene structure. J Fluoresc34:275–281. https://doi.org/10.1007/s10895-023-03256-6.

[3]. Shivaleela B, Shivraj G. G. and S. M. Hanagodimath, "Estimation of Dipole Moments by Solvatochromic Shift Method, Spectroscopic Analysis of UV-Visible, HOMO-LUMO, ESP Map, Mulliken Charges, NBO And NLO Properties of Benzofuran Derivative" Results in Chemistry, Vol 6, Dec 2023, 101046. https://doi.org/10.1016/j.rechem .2023.101046

[4]. H.R. Deepa, S. Chandrasekhar, J. Thipperudrappa, Chem. Phys. Impact4(2022), 100075.

[5]. Poronik YM, Baryshnikov GV, Deperasinska I, Espinoza EM, Clark JA, Ågren H, Gryko DT, Vullev VI (2020) Deciphering the unusual fluorescence in weakly coupled bis-nitro-pyrrolo[3,2- ] pyrroles. Communications Chemistry 3. https://doi.org/ARTN.19010.1038 /s42004-020-00434-6.

[6]. S. Chandrasekhar, H.R. Deepa, R.M. Melavanki, S. Moguram pelly, M.M.Basanagouda, J.Thipperudrappa, S. Yallappa, Chem. Data Collect.29(2020),100516.

[7]. S. Chandrasekhar, H.R. Deepa, R. Melavanki, M.M. Basanagou da, S. Mogurampelly, J. Thipperudrappa, Luminescence.36(2021) 769–787

[8]. Prajakta S. Kadolkar, Shivaraj A. Patil, Wari, Sanjeev R. Inam dar j.molliq.2020.113452.

[9]. Shivaleela B. and S.M.Hanagodimath, "Quantum chemical calculations on NBO, NLO, Spectroscopic (UV-Visible, IR, Raman, 1H and 13C NMR) analysis, HOMO-LUMO and ESP map of fluorescent molecule by Semi-empirical and Hartree-Fock optimization methods, Journal of International Academy of Physical Sciences, Vol 27, 1(2023), 69-78.

[10]. L.C. Luz, M.G. Gündüz, R. Beal, G.M. Zanotto, E.R. Kuhn, P.A. Netz, C. S¸ afak, P.F.B. Gonçalves, Fabiano da silveira santos, fabiano severo rodembusch, J Photochem. Photobiol. 429 (2022),113915.

[11]. Mallikarjun, K. Patil, M.G. Kotresh, Sanjeev R. Inamdar, https://doi .org/10.1016/j.saa.2019.02.022

[12]. Shivaraj A. Patil, Prajakta S. Kadolkar, Manjunath, N. Wari, Sanjeev, R. Inamdar, S2352492821007248.

[13]. J. Thipperudrappa, D.S. Biradar, M.T. Lagare, S.M. Hanagodimath, S. R. Inmdar, S J.S. Kadadevaramath, https://doi.org/10.1016/j.jph otochem.2005.05.016

[14]. K. Vibha a, N.C. Prachalith a , R. Annoji Reddy a,b , M.N. Ravikantha a,c , J. Thipperudrappa a, [15]. M. K. Patil, M.G. Kotresh, S.R. Inamdar, Spectrochimica ActaPart A, DOI: S1386–1425(19)30134–9. https://doi.org/10.1016/j.saa.2019.02.022.

[15]. N. Sunil Kumar a , K.N.N. Prasad b,* , S. Chandrasekhar b , J. Thipp erudrappa c, sciencedirectassets.com, https://doi.org/10.1016/j.ch phi.2022.100136

[16]. Jing Han W, Chih-Ling C, Zhe Wei Z, Mahdy EL, Ahmed FM (2022) Facile metal-free synthesis of pyrrolo[3,2-b] pyrrolyl based conjuga ted microporous polymers for high-performance photocatalytic degra dation of organic pollutants. Polym Chem 13:37:5300–5308.https://d oi.org/10.1039 /d2py00658h

[17]. Bhardwaj K, Anand T, Jangir R, Sahoo SK (2024) Aggregation Induced emission active Benzidine-Pyridoxal derived scaffold for detecting Fe(3+) and pH. J Fluoresc 34:2917–2926. https://doi.org/10.1007/s1 0895-023-03503-w.

[18]. HA.Z. Sabek, AM.M. Alazaly, D. Salah, HS. Abdel-Samad, MA. Ismail,A.A. Abdel- Shafi, RSC Adv. 10 (2020) 43459–4 3471.

[19]. S.N. Saravanamoorthy, G. Sathiyapriya, M. Sivasakthi, Int. J. Res. Appl. Sci. Eng. Technol. 7 (2019) 1017–1028 (IJRASET).

[20]. Mahesh, S. Najare , Mallikarjun K. Patil, Afra Quasar A. Nadaf, Shivaraj Mantur, Manjunatha Garbhagudi, Supreet Gaonkar, Sanjeev R. Inamdar, Imtiyaz Ahmed M. Khazi j.molstruc.2019.127032.pdf

[21]. S.K. Patila, M.N. Warib, C. Yohannan Panickerc, Inamdar, j.saa.2013 .12.031.pdf

[22]. Airin Antony, J.Mitra, Refractive index-assisted UV/Vis spectrophotometry to overcome spectral interference by https://www.sciencedirect.com/science/article/abs/pii/S0003267 020312691,

[23]. A. Frisch, R. Dennington, T. Keith, J. Millam, A. Nielsen, A.J. Holder, Hiscocks, Gauss View Version 5 User Manual, Gaussian Inc, Wallingford, CT, USA,2009.

[24]. Shivaleela B. and S. M. Hanagodimath, "Studies on molecular structure, UV-Visible and HOMO-LUMO analysis of coumarin dye using DFT computational methods", in AIP Conference Proceedings, Vol. 269, No. 1, 13th Sep 2021, p.020151.https://doi.org/10.1063/5.0060877

[25]. Y.F. Nadaf, B.G. Mulimani, M. Gopal, Inamdar, j.theochem. 2004.01.049.pdf

[26]. Hawks AM, Altman D, Faddis R, Wagner EM, Bell KJ, Charland Martin A, Collier GS (2023) Relating design and optoelectronic properties of 1,4- Dihydropyrrolo [3,2-b] pyrroles bearing biphenyl substituents. J Phys Chem B 127:7352–7360. https://doi.org/10. 1021/acs.jpcb.3c03061.

[27]. Hawks AM, Daniel LM, Sorto VS, Mauro J, Skiouris P, Collier GS (2024) Expanding color control of anodically coloring electrochromes based on Electron-Rich 1,4-Dihydropyrrolo [3,2-b] pyrroles. ACS Appl Opt Mater 2:1235–1244.https://doi.org/10.1021/acsaom.4c00 197

[28]. Radha Goudar, Ritu Gupta, Giridhar U. Kulkarni, Sanjeev R. Inamdar, J. Fluoresc.25(2015) 1671–1679, https://doi.org/10.1007/s10895-015-1654-6.

[29]. V.V. Koppal, Raveendra Melavanki, Raviraj Kusanur, N.R. Patil, Analysis of Fluorescence Quenching of Coumarin Derivative under Steady State and Transient State Methods, https://doi.org/10.100 7/s10895-020-02663-3

[30]. S.P. Olivares, S.Risso, M.I. Gutie´rrez, Spectrochim. ActaA71(2008)336–339

[31]. S.K.Patila, M.N.Warib, C.Yohannan Panickerc,S.R. Inamdarb, j.saa.2013.12.031.pdf.

[32]. J.A. Dean, Lange'sHandbookofChemistry,15thed., McGraw-Hill, New York, 1999

[33]. J.R. Lackowicz, Principles of Fluorescence Spectroscopy, Plenum Press, New York, 1983.z

[34]. M.J. Kamlet, J.L.M. Abboud, M.H. Abraham, R.W. Taft, J. Org. Chem. 48 (1983)2877–2887.

[35]. M.J. Kamlet, Prog. Phys.Org.Chem.13(1982)485.

[36]. R.B. da Silva, F. Lange Coelho, F.S. Rodembusch, R.S. Schwab, J.M.F.M. Schneider,D. da Silveira Rampon, P.H. Schneider, New J. Chem. 43 (2019) 11596–11603.

[37]. Sanjeev,R.Inamdar,James, R. Mannekutla, M.S.Sannaikar, M. N. Wari, B.G. Mulimani, M. I. Savadatti, https://doi.org/10.1016/j.molliq .2018.07.005

[38]. G.H. Pujar, M.N. Wari, B. Steffi, H. Varsha, B. Kavita, C. Yohannan Panicker, http://dx.doi.org/10.1016/j.molliq.2017.08.078

[39]. Jana Basavaraja, S.R. Inamdar, H.M. Suresh Kumar j.saa.2016.07.010. pdf

[40]. M.J. Kamlet, J.L. Abboud, R.W. Taft, J.Am.Chem.Soc.99 (1977)6027–6038